Journal of Biomechanics 42 (2009) 587–593

Contents lists available at ScienceDirect

Journal of Biomechanics

journal homepage: www.elsevier.com/locate/jbiomech
www.JBiomech.com

Thigh–calf contact: Does it affect the loading of the knee in the high-flexion range?

J. Zelle [a,*], M. Barink [a], M. De Waal Malefijt [a], N. Verdonschot [a,b]

[a] Orthopaedic Research Laboratory, Radboud University Nijmegen Medical Center, P.O. Box 9101, 6500 HB Nijmegen, The Netherlands
[b] Laboratory for Biomechanical Engineering, University of Twente, Enschede, The Netherlands

ARTICLE INFO

Article history:
Accepted 16 December 2008

Keywords:
Total knee arthroplasty
High-flexion
Thigh–calf contact
Squatting
Kneeling
Finite element analysis

ABSTRACT

Recently, high-flexion knee implants have been developed to provide for a large range of motion (ROM > 120°) after total knee arthroplasty (TKA). Since knee forces typically increase with larger flexion angles, it is commonly assumed that high-flexion knee implants are subjected to larger loads than conventional knee implants. However, most high-flexion studies do not consider thigh–calf contact which occurs during high-flexion activities such as squatting and kneeling. In this study, we hypothesized that thigh–calf contact reduces the knee forces during deep knee flexion as the tibio-femoral load shifts from occurring inside the knee towards the thigh–calf contact interface. Hence, the effect of thigh–calf contact on the knee loading was evaluated using a free body diagram and a finite element model and both the knee forces and polyethylene stresses were analyzed. Thigh–calf contact force characteristics from an earlier study were included and a squatting movement was simulated. In general, we found thigh–calf contact considerably reduced both the knee forces and polyethylene stresses during deep knee flexion. At maximal flexion (155°), the compressive knee force decreased from 4.89 to 2.90 times the bodyweight (BW) in case thigh–calf contact was included and the polyethylene contact stress at the tibial post decreased from 49.3 to 28.1 MPa. Additionally, there was a clear correlation between a subject's thigh and calf circumference and the force reduction at maximal flexion due to thigh–calf contact ($R = 0.89$). The findings presented in this study can be used to optimize the mechanical behavior of high-flexion total knee arthroplasty designs.

1. Introduction

Total knee arthroplasty (TKA) is a successful surgical procedure having good to excellent survival rates of roughly 95% after 10 yr (Buehler et al., 2000; Khaw et al., 2001; Fetzer et al., 2002). Due to the success of TKA, patients receiving a total knee replacement are currently younger and more active than patients in the past and post-operative range of motion (ROM) has become more important. So-called high-flexion knee implants have been developed to provide for a larger flexion range (ROM > 120°) after TKA than conventional implants (ROM ⩽ 120°). High-flexion designs are often based on successful conventional designs and have been adapted to endure the more extreme loading conditions occurring during high-flexion (Nagura et al., 2002; Nagura et al., 2006). Since its recent introduction a wide variety of high-flexion implants have been developed such as the Sigma RP-F (Depuy, Warsaw, IN), the Nexgen LPS Flex (Zimmer, Warsaw, IN), the Scorpio Flex (Stryker, Kalamazoo, MI), the Genesis II High Flex (Smith & Nephew, Memphis, TN) and the Vanguard CKS (Biomet, Warsaw, IN).

Finite element (FE) analysis is a good method to analyze knee mechanics. FE models have been used to investigate patello-femoral (D'Lima et al., 2003; Besier et al., 2005) and tibio-femoral contact mechanics (D'Lima et al., 2001; Godest et al., 2002; Taylor and Barrett, 2003; Halloran et al., 2005). Recently, also high-flexion knee mechanics have been simulated using FE models (Morra and Greenwald, 2005; Barink et al., 2008). Obviously, the outcome of FE studies heavily depends on input parameters such as joint and muscle forces. Joint forces are often estimated by musculo-skeletal models using inverse dynamics. Knee forces reported in the literature differ noticeably and range from 2 to 7 times the bodyweight (BW) during deep knee flexion (Dahlkvist et al., 1982; Escamilla et al., 1998; Komistek et al., 2005; Nagura et al., 2006). Prior FE studies typically show higher knee forces and polyethylene stresses with increasing flexion angles. Morra and Greenwald (2005) analyzed polyethylene loadings during several high-flexion activities. For various implant designs they demonstrated plastic deformation during a kneel-rise activity which was simulated using a compressive joint load of 4.4 × BW (135° of flexion).

* Corresponding author. Tel.: +31 24 3617099.
E-mail address: J.Zelle@orthop.umcn.nl (J. Zelle).

0021-9290/$ - see front matter © 2009 Elsevier Ltd. All rights reserved.
doi:10.1016/j.jbiomech.2008.12.015

A substantial part of the knee patients receiving a total knee replacement routinely perform deep knee flexion activities. Weiss et al. (2002) demonstrated that 40% of the Western knee patient population included in their study performed high-flexion activities such as squatting, kneeling and gardening on a regular basis (more than twice per week). In addition, the orthopaedic market is flourishing in Asia and the Middle East where many activities are performed while squatting or kneeling (Mulholland and Wyss, 2001). During such high-flexion activities posterior contact between the thigh and the calf occurs (Fig. 1). Currently, there is no knee model which includes thigh–calf contact occurring during deep knee flexion. Thigh–calf contact may well reduce the loading of the knee as the tibio-femoral load transfer shifts from occurring inside the knee to the thigh–calf contact interface.

In an earlier study, we measured the thigh–calf contact load transfer using 10 healthy subjects and we demonstrated that thigh–calf contact is substantial during squatting: ±35% BW on each leg (Zelle et al., 2007). In the current study, the effect of thigh–calf contact on the knee loading was studied using the contact characteristics measured previously. We hypothesized that thigh–calf contact reduces the loading of the knee during high-flexion as the joint load shifts from occurring inside the knee to the thigh–calf contact interface. Firstly, we analyzed the effect of thigh–calf contact at a global level by studying the knee force patterns using a free body diagram (FBD). Thigh–calf contact characteristics of a typical subject were incorporated in this model. Secondly, thigh–calf contact characteristics of all subjects measured earlier were included in the FBD to analyze correlations between corpulence-related properties and the resulting joint forces. Finally, the effect of thigh–calf contact was studied on a more detailed basis by evaluating the loading of a polyethylene TKA component using a dynamic FE knee model.

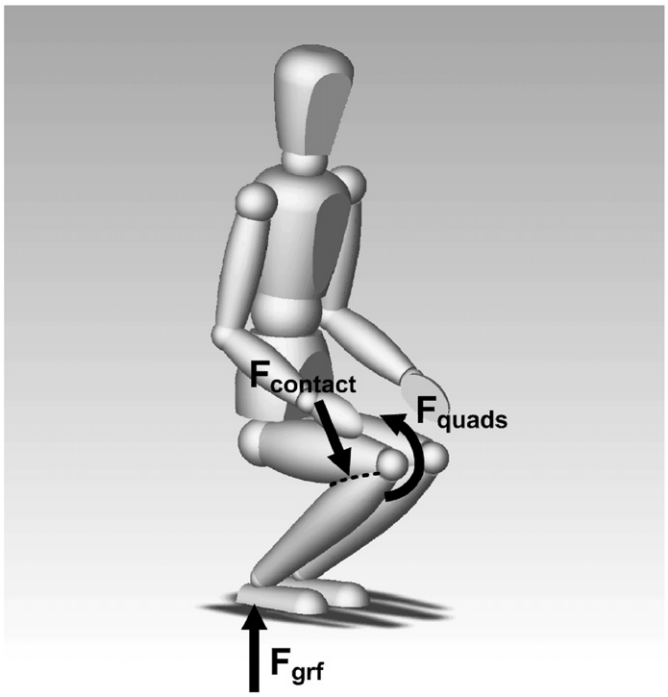

Fig. 1. Thigh–calf contact occurring during a high-flexion squatting activity. The ground reaction force (F_{grf}) produces a flexion moment around the knee joint. Consequently, the quadriceps muscle (F_{quads}) has to exert an extension moment around the knee to maintain the equilibrium. Thigh–calf contact ($F_{contact}$) limits knee flexion and generates an extension moment around the knee. Hence, in case thigh–calf contact occurs the quadriceps muscle force is reduced.

2. Material and methods

The effect of thigh–calf contact on the prosthetic knee loading was analyzed during squatting using both an FBD and an FE model of the human knee. Thigh–calf characteristics of a typical subject were included in both models to evaluate this effect.

2.1. Typical thigh–calf contact characteristics

The resultant thigh–calf contact force and its location on the tibia of a typical subject having a standard body mass (BM = 78 kg), body length (BL = 1.87 m) and body mass index (BMI = 22.3 kg/m^2) were obtained from earlier thigh–calf contact force measurements (Zelle et al., 2007). For use in this study, the resultant thigh–calf contact force F_{tc} (in percentage BW) and the contact force location on the tibia L_{tc} (in meters) were expressed as functions of the knee flexion angle α (in degrees) using a polynomial data-fitting technique

$$F_{tc} = 4.7133 \times 10^{-2}\alpha^2 - 12.256\alpha + 798.68 \quad (1)$$

$$L_{tc} = 6.9596 \times 10^{-6}\alpha^3 - 2.8729 \times 10^{-3}\alpha^2 + 0.39584\alpha - 18.088 \quad (2)$$

Note that these equations apply to a flexion range of 125–155° of flexion as thigh–calf contact initiated at 125° of flexion for this typical subject and the maximal flexion angle the subject achieved was 155° of flexion.

2.2. Free body diagram

A two-dimensional sagittal FBD of the knee was developed to explore the effect of thigh–calf contact on the knee forces during knee flexion. Initially, the FBD of the lower limb was generated using a cut section through the knee joint (Fig. 2). Several assumptions were made to simplify the FBD and the thigh–calf contact analysis. Firstly, heel–ground contact was assumed during the squatting movement and the ground reaction force was considered to be constant in magnitude (350 N) and to act through the ankle joint. Secondly, the hamstrings and gastrocnemius muscle were neglected since considerably lower forces have been reported for this muscle during squatting in comparison with the quadriceps muscle (Dahlkvist et al., 1982). Thirdly, the collateral ligaments were neglected since they have little effect on the knee mechanics in the sagittal plane (Crowninshield et al., 1976; Zheng et al., 1998). Finally, both cruciate ligaments were excluded as these ligaments are sacrificed during the posterior stabilized TKA as analyzed in this study (PFC Sigma RP-F). The lengths of the tibia and femur were taken from the CT-scan upon which the FE model used in this study was based (next paragraph). The orientation of the patella tendon and its moment arm were obtained from the simulations with the same FE model and matched values reported in literature (Van Eijden et al., 1986; Kellis and Baltzopoulos, 1999). The accelerations of the segments were considered to be low as a relatively slow squatting activity was simulated in this study. All assumptions listed were integrated in the FBD which resulted in the static equilibrium equations given

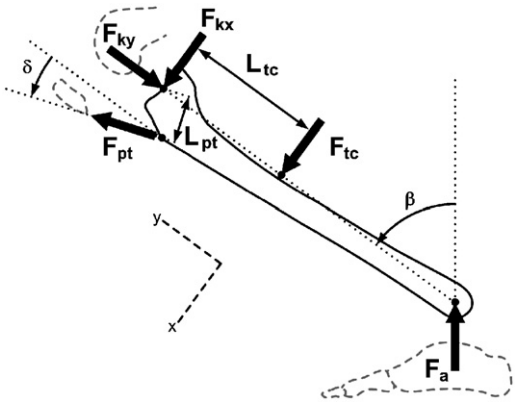

Fig. 2. Free body diagram of the lower limb in the sagittal plane containing the following forces and moment arms: the ankle force (F_a), the patella tendon force (F_{pt}), the resultant thigh–calf contact force (F_{tc}), the knee joint forces (F_{kx} and F_{ky}), the patella tendon moment arm (L_{pt}) and the thigh–calf contact moment arm (L_{tc}). The ankle force is directed towards the hip joint. β is the angle between the vertical and the tibial axis and was derived from the knee flexion angle using the cosinus rule and δ is the orientation of the patella tendon with respect to the tibial axis.

below (Fig. 2)

$$\sum F_x = 0 \quad \rightarrow F_{kx} + F_{pt} \sin \delta - F_a \sin \beta + F_{tc} = 0 \tag{3}$$

$$\sum F_y = 0 \quad \rightarrow F_{pt} \cos \delta + F_a \cos \beta - F_{ky} = 0 \tag{4}$$

$$\sum M_k = 0 \quad \rightarrow F_{pt} L_{pt} + F_{tc} L_{tc} - (F_a \sin \beta) L_{tib} = 0 \tag{5}$$

Knee forces were computed during a downward squatting movement (ROM = 50–155°) both with and without typical thigh–calf contact included, respectively (Eqs. (1) and (2)). Three different knee forces were examined to study the effect of thigh–calf contact: the compressive knee force, the shear knee force and the patella tendon force. All joint forces were normalized for BW.

The FBD was furthermore utilized to study correlations between corpulence-related subject properties and the resulting knee forces. These correlations provide information of how the outcome of this study is to be applied to standard knee patients who typically have a higher BMI than the healthy subjects considered in the earlier study. Hence, subject-specific knee forces were computed using the FBD and the individual thigh–calf contact characteristics measured earlier. The magnitude of the compressive and shear knee force reduction due to thigh–calf contact were normalized for BW for all subjects and evaluated at 150° of flexion which was the maximal flexion angle most subjects achieved (one subject was excluded). Correlations were determined between the BMI and the sum of thigh and calf circumference of the subjects and the knee force reduction due to thigh–calf contact using the Pearson's linear correlation coefficient for a 95% confidence interval.

2.3. Finite element model

A three-dimensional dynamic FE model of a prosthetic knee was used to evaluate the implications of thigh–calf contact on the polyethylene stresses during high-flexion. The FE model utilized in this study has previously been developed in the FE program Marc (MSC Software Corporation, Santa Ana, CA). The model consisted of a distal femur, a proximal tibia and fibula, TKA components, a quadriceps and patella tendon and a non-resurfaced patella (Fig. 3).

A detailed model description has been supplied earlier (Barink et al., 2008). However, a short summary of the most important features is given here. High-flexion components of the posterior stabilized PFC Sigma RP-F (Depuy International, Leeds, UK) were integrated following the surgical procedure provided by the manufacturer. Hexahedral (brick) elements were used to model all bones and components, except the femoral component, which was modeled as a rigid body. In general, linear material models were used for all components, except for the polyethylene, which was modeled as an elastic–plastic non-linear material having an initial yield stress of 14 MPa (Kurtz et al., 1998). Both the quadriceps and patella tendon were included and modeled as composite materials consisting of shell elements and non-linear line elements to represent the solid matrix and collagen fibers of these ligaments. Collateral and cruciate ligaments were not ignored for similar reasons as mentioned in the FBD description (previous paragraph). Tibio-femoral and patello-femoral contact were defined and the quadriceps tendon was able to wrap around the femoral component. Knee flexion was simulated by application of the ground reaction force similar to the FBD and releasing the quadriceps tendon incrementally.

Polyethylene stresses were computed using the FE model during a downward squatting movement (ROM = 50–155°) both with and without typical thigh–calf contact characteristics included, respectively (Eqs. (1) and (2)). Three knee forces (the compressive, shear and patella tendon force) were determined using the FE model to assess whether these were concurrent with those predicted by the FBD. Furthermore, three polyethylene loading-related parameters were studied: the equivalent Von Mises stress, the contact (normal) stress and the volume fraction of the polyethylene participating in plastic deformation.

3. Results

3.1. Free body diagram

Thigh–calf contact considerably reduced the joint forces during high-flexion (Fig. 4a). The compressive knee force at maximal flexion (155°) calculated by the FBD decreased from 4.37 to 3.07 × BW and the shear knee force at maximal flexion reduced from 1.31 to 0.72 × BW. In general, the maximal joint forces shifted from occurring at maximal flexion to the initiation angle of thigh–calf contact at ±130° of flexion in case thigh–calf contact was included in the analyses.

Significant correlations were found between the sum of the thigh and calf circumference and the knee force reduction due to thigh–calf contact (Fig. 5b) at the maximal flexion angle achieved by all subjects (150°) for both the compressive force ($R = 0.89$; $P = 0.0015$) and the shear force ($R = 0.87$; $P = 0.0022$). Correlations between the BMI of the subjects (Fig. 5a) and the reduction in knee forces due to the posterior soft-tissue compression were less clear for both the compressive force ($R = 0.68$; $P = 0.046$) and the shear force ($R = 0.67$; $P = 0.050$).

3.2. Finite element model

The joint forces computed by the FE model (Fig. 4b) were in good agreement with those computed by the FBD model (Fig. 4a). The compressive and shear knee force as well as the patella tendon force were comparable in trend and magnitude in both computations. For computations with the FE model, the compressive knee force at maximal flexion (155°) decreased from 4.89 to 2.90 × BW and the shear knee force at maximal flexion reduced from 0.95 to 0.41 × BW.

As a consequence of the lower knee forces the FE predictions demonstrated that thigh–calf contact had a considerable effect on the prosthetic mechanics. Both the polyethylene Von Mises stress

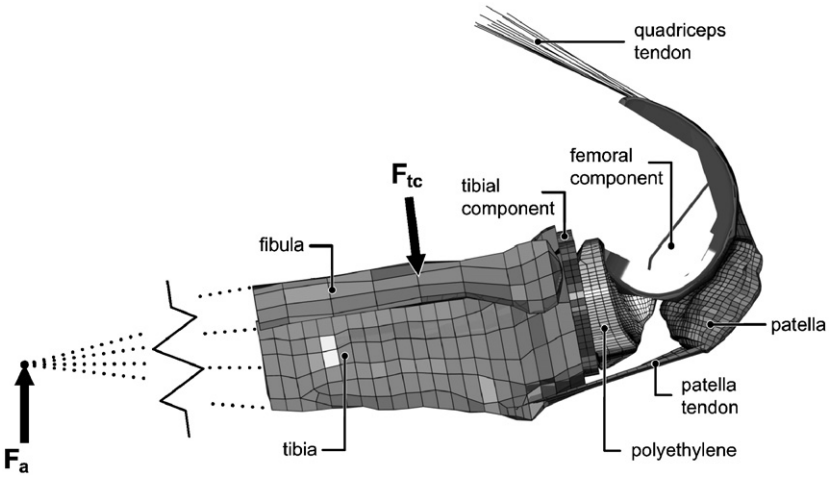

Fig. 3. The dynamic FE model utilized in this study. The model contains bones (the fibula, tibia and patella), TKA components and external loads (the ankle load F_a and thigh–calf contact F_{tc}). Flexion was simulated by applying the ankle force (directed towards the hip joint) and releasing the quadriceps tendon slightly per increment.

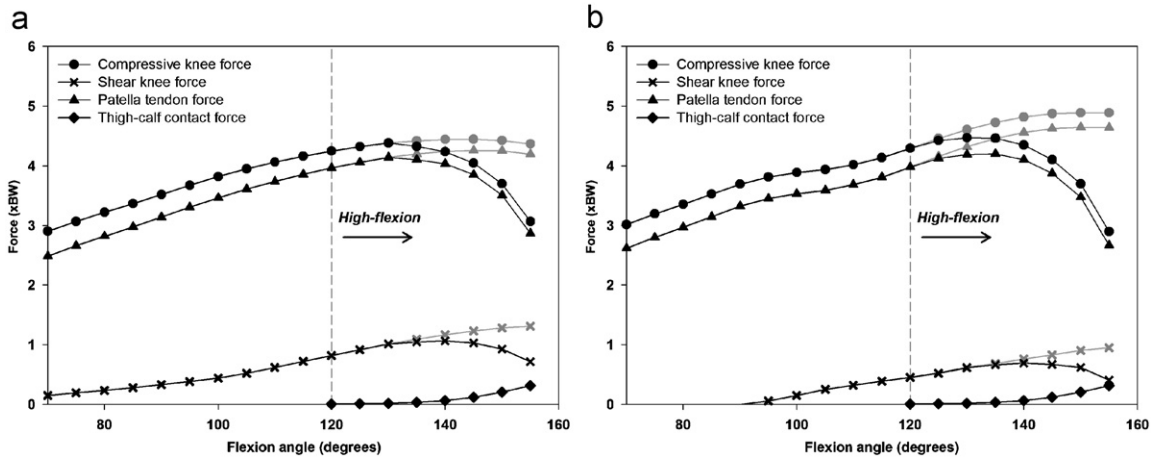

Fig. 4. Joint forces normalized for BW computed by the FBD (a) and the FE model (b). The black curves characterize the calculations with thigh–calf contact included and the grey curves with no thigh–calf contact included.

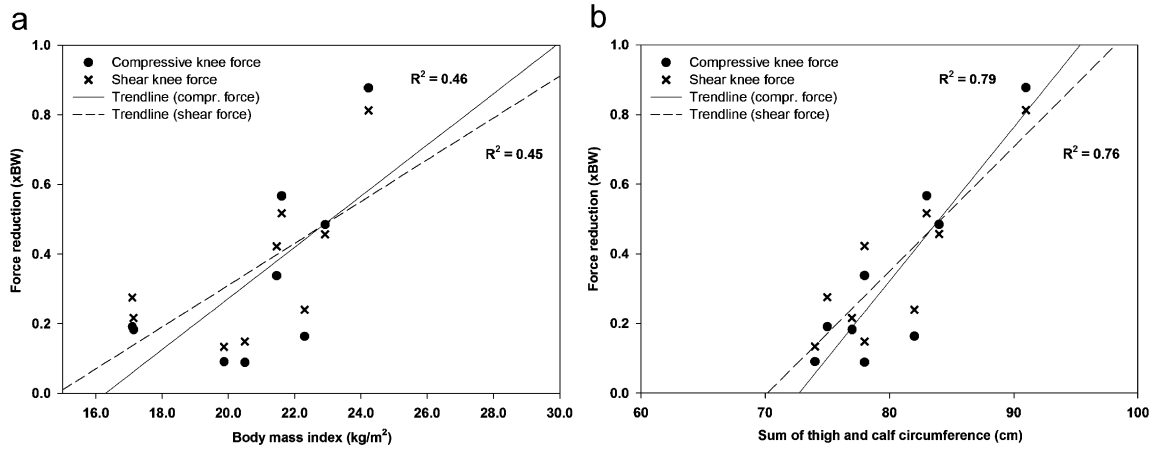

Fig. 5. Correlation plots of the body mass index (a) and the sum of circumferences of thigh and calf (b) versus the knee force reduction due to thigh–calf contact at 150° of flexion for all the subjects (BM range = 50.0–95.0 kg; BMI range = 17.1–24.2 kg/m^2).

and contact stress decreased considerably at maximal flexion when thigh–calf contact was included (Fig. 6). The Von Mises stresses reached peak values of 29 MPa at the post during simulations with and without thigh–calf contact. However, at maximal flexion, the maximal Von Mises stress decreased from 29.08 to 25.89 MPa at the dish and decreased from 24.83 to 15.86 MPa at the post due to thigh–calf contact. Similar results were obtained for the maximal contact stress. At maximal flexion, the maximal contact stress decreased from 58.13 to 53.82 MPa at the dish and decreased from 49.32 to 28.06 MPa at the post.

Plastic deformation of the polyethylene reduced in case thigh–calf contact was included in the model (Fig. 7). In case no thigh–calf contact was assumed, the polyethylene volume fraction involved in plastic deformation gradually increased after 130° of flexion, whereas plastic deformation did not further accumulate during high-flexion in case thigh–calf contact was included. At maximal flexion (155°), the volume fraction participating in plastic deformation reduced from 10.3% to 8.64% due to thigh–calf contact.

4. Discussion

To the authors knowledge this study is the first effort to describe the effect of thigh–calf contact on the knee loading. Although the knee models described in this study are expected to be representative for the in-vivo situation, the models contain several assumptions which possibly affected the outcome. The maximal compressive knee force computed for squatting in this study corresponds to values reported earlier which range between 2 and 7 × BW (Dahlkvist et al., 1982; Escamilla et al., 1998; Komistek et al., 2005; Nagura et al., 2006). However, recent studies focusing only on heels-down squatting report lower values of 2 to 3 × BW (Toutoungi et al., 2000; Thambyah, 2008; Smith et al., 2008). One major assumption we made in this study was heels-down squatting during which the ground reaction force was assumed to act through the ankle joint. Hence, the knee flexion moment resulting from the ground reaction force was relatively high compared to other studies where the ground reaction force was located more anterior during the heels-down squatting motion (Thambyah, 2008). The knee flexion moment is furthermore influenced by anatomical parameters such as segment lengths and tendon moment arms and the amount of muscles described in the model. Due to the fact that we analyzed heels-down squatting and the ankle force acted through the ankle joint, the forces generated by the calf muscles (soleus and gastrocnemius) were neglected. Heels-down squatting is a common posture in Asian countries (Hemmerich et al., 2006) which is an important high-flexion TKA market. In case we would have considered heels-up squatting, which is probably more common

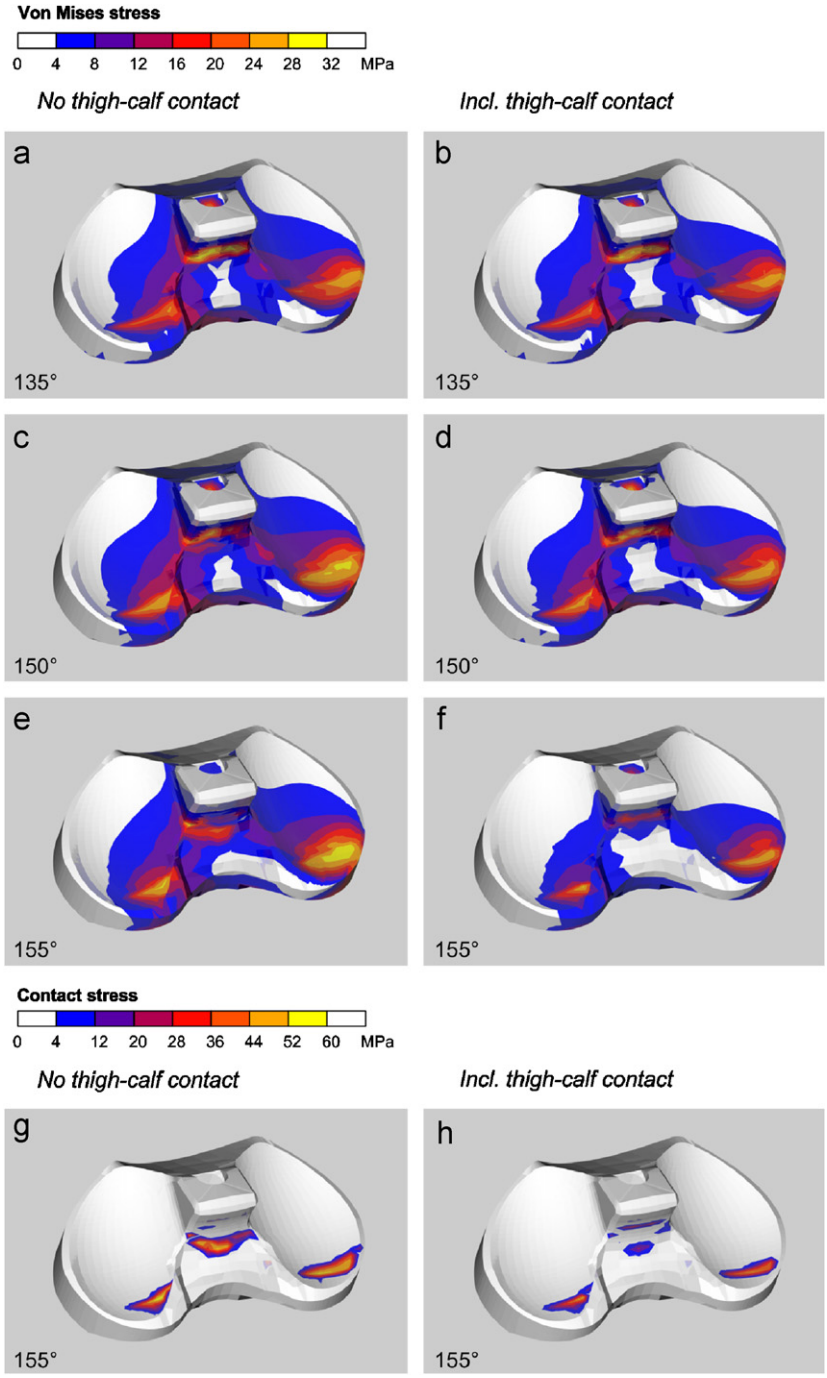

Fig. 6. Material stresses in the polyethylene at three different flexion angles: 135° (a and b), 150° (c and d) and 155° (e–h). Figures on the left are obtained from simulations with no thigh–calf contact and figures on the right from simulations with thigh–calf contact included.

in Western countries, the force generated by mainly the gastrocnemius muscle would have an increasing effect on the general knee load. Overall, the joint force trends as described in this study are comparable to other studies (Smith et al., 2008) and most likely thigh–calf contact has a similar effect during other deep squatting postures regardless the exact joint force magnitude.

There was a clear correlation between the sum of thigh and calf circumference and the resulting knee force reduction due to thigh–calf contact. Large thigh and calf circumferences promote the initiation of soft-tissue contact during deep knee flexion which results in a larger force reduction at maximal flexion. Hence, if the results of this study were to be applied to Western knee patients who typically have a high BMI (Gupta et al., 2006) and obese leg segments, these knee patients would benefit relatively more from the contact between thigh and calf during high-flexion. Bodyweight is related to obesity and an increase of the thigh and calf circumference implicates an increase in bodyweight and the global level of knee forces. The current study shows that thigh–calf contact can (partly) compensate for this force increase.

Thigh–calf contact considerably reduces the knee forces at maximal flexion as demonstrated in this study. However, the

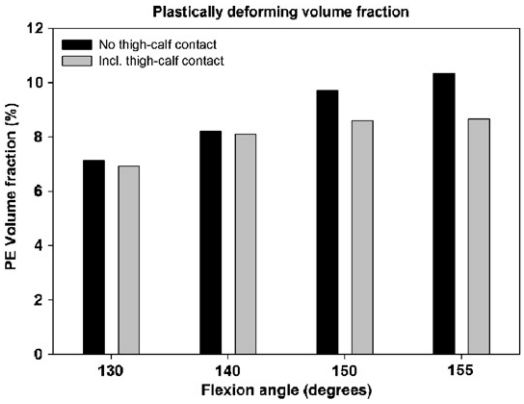

Fig. 7. Polyethylene volume fraction participating in plastic deformation in case thigh–calf contact was included or excluded during high-flexion.

global magnitude of the knee forces occurring during the entire flexion cycle was only slightly reduced by thigh–calf contact. For instance, the peak compressive knee force decreased from 4.45 to 4.38 × BW and 4.89 to 4.47 × BW computed by the FBD and FE model, respectively. Hence, the main point of this study is that high-flexion designs are based on the assumption that the highest forces are generated at maximal flexion angles. This study clearly shows that this assumption is not valid and that design criteria may need to be altered accordingly. The outcome of the current study supports the hypothesis that the knee loads might not be as high as generally expected at maximal flexion. Therefore, reinforcement of high-flexion implants (e.g. metal pin in the tibial post in case of the Sigma RP-F) is questionable as conventional implants are often not reinforced and both implant types experience similar loads. In addition, since the highest forces did not occur during maximal flexion, but at lower flexion angles of approximately 130° of flexion, tibio-femoral contact has to be optimized for these flexion angles to minimize polyethylene wear.

The maximal Von Mises stress of 29 MPa encountered in this study was comparable to values found in literature. D'Lima et al. (2001) computed a maximal Von Mises stress of 30 MPa using an axial tibial load of 3000 N (0° of flexion). Morra and Greenwald (2003) found a maximal Von Mises stress of 26 MPa in case a compressive tibio-femoral force of 2340 N (15° of flexion) was applied. Plastic deformation of the polyethylene insert was observed in this study during high-flexion which has also been shown by Morra and Greenwald (2005). Post-cam contact stresses reached peak values of 70 MPa in case thigh–calf contact was included (shear knee force = 0.7 × BW). The actual value of the peak contact stress is difficult to compare with other studies as it depends on the material model incorporated as well as the mesh density and the contact algorithm used. In general, polyethylene contact stresses reported in other studies are lower than described in this study. Morra and Greenwald (2005) computed a maximal contact stress of 32 MPa at the post using a shear knee force of 0.4 × BW (135° of flexion). Huang et al. (2006) computed a maximal contact stress of 59 MPa at the post using a shear force of 500 N (150° of flexion). For this purpose, we mainly evaluated the qualitative effect of thigh–calf contact and outcome differences between different simulations.

In conclusion, the current study confirms that thigh–calf contact reduces the knee forces in the high-flexion range. Both the joint forces and the polyethylene stresses reduced considerably when thigh–calf contact was included. The findings presented in this study can be used to optimize the mechanical behavior of high-flexion TKA designs.

Conflicts of interest

The authors declare that they have no competing interests.

Acknowledgement

This research was made possible by a research grant from Depuy International Ltd., Leeds, UK.

References

Barink, M., De Waal, M.M., Celada, P., Vena, P., Van, K.A., Verdonschot, N., 2008. A mechanical comparison of high-flexion and conventional total knee arthroplasty. Proc. Inst. Mech. Eng. (H) 222, 297–307.
Besier, T.F., Gold, G.E., Beaupre, G.S., Delp, S.L., 2005. A modeling framework to estimate patellofemoral joint cartilage stress in vivo. Med. Sci. Sports Exerc. 37, 1924–1930.
Buehler, K.O., Venn-Watson, E., D'Lima, D.D., Colwell Jr., C.W., 2000. The press-fit condylar total knee system: 8- to 10-year results with a posterior cruciate-retaining design. J. Arthroplasty 15, 698–701.
Crowninshield, R., Pope, M.H., Johnson, R.J., 1976. An analytical model of the knee. J. Biomech. 9, 397–405.
D'Lima, D.D., Chen, P.C., Colwell Jr., C.W., 2001. Polyethylene contact stresses, articular congruity, and knee alignment. Clin. Orthop. Relat. Res., 232–238.
D'Lima, D.D., Chen, P.C., Kester, M.A., Colwell Jr., C.W., 2003. Impact of patellofemoral design on patellofemoral forces and polyethylene stresses. J. Bone Joint Surg. Am. 85 (4), 85–93.
Dahlkvist, N.J., Mayo, P., Seedhom, B.B., 1982. Forces during squatting and rising from a deep squat. Eng. Med. 11, 69–76.
Escamilla, R.F., Fleisig, G.S., Zheng, N., Barrentine, S.W., Wilk, K.E., Andrews, J.R., 1998. Biomechanics of the knee during closed kinetic chain and open kinetic chain exercises. Med. Sci. Sports Exerc. 30, 556–569.
Fetzer, G.B., Callaghan, J.J., Templeton, J.E., Goetz, D.D., Sullivan, P.M., Kelley, S.S., 2002. Posterior cruciate-retaining modular total knee arthroplasty: a 9- to 12-year follow-up investigation. J. Arthroplasty 17, 961–966.
Godest, A.C., Beaugonin, M., Haug, E., Taylor, M., Gregson, P.J., 2002. Simulation of a knee joint replacement during a gait cycle using explicit finite element analysis. J. Biomech. 35, 267–275.
Gupta, S.K., Ranawat, A.S., Shah, V., Zikria, B.A., Zikria, J.F., Ranawat, C.S., 2006. The P.F.C. sigma RP-F TKA designed for improved performance a matched-pair study. Orthopedics 29, S49–S52.
Halloran, J.P., Petrella, A.J., Rullkoetter, P.J., 2005. Explicit finite element modeling of total knee replacement mechanics. J. Biomech. 38, 323–331.
Hemmerich, A., Brown, H., Smith, S., Marthandam, S.S., Wyss, U.P., 2006. Hip, knee, and ankle kinematics of high range of motion activities of daily living. J. Orthop. Res. 24, 770–781.
Huang, C.H., Liau, J.J., Huang, C.H., Cheng, C.K., 2006. Influence of post-cam design on stresses on posterior-stabilized tibial posts. Clin. Orthop. Relat. Res. 450, 150–156.
Kellis, E., Baltzopoulos, V., 1999. In vivo determination of the patella tendon and hamstrings moment arms in adult males using videofluoroscopy during submaximal knee extension and flexion. Clin. Biomech. (Bristol, Avon.) 14, 118–124.
Khaw, F.M., Kirk, L.M., Gregg, P.J., 2001. Survival analysis of cemented press-fit condylar total knee arthroplasty. J. Arthroplasty 16, 161–167.
Komistek, R.D., Kane, T.R., Mahfouz, M., Ochoa, J.A., Dennis, D.A., 2005. Knee mechanics: a review of past and present techniques to determine in vivo loads. J. Biomech. 38, 215–228.
Kurtz, S.M., Ochoa, J.A., White, C.V., Srivastav, S., Cournoyer, J., 1998. Backside nonconformity and locking restraints affect liner/shell load transfer mechanisms and relative motion in modular acetabular components for total hip replacement. J. Biomech. 31, 431–437.
Morra, E.A., Greenwald, A.S., 2003. Effects of walking gait on ultra-high molecular weight polyethylene damage in unicompartmental knee systems, a finite element study. J. Bone Joint Surg. Am. 85 (4), 111–114.
Morra, E.A., Greenwald, A.S., 2005. Polymer insert stress in total knee designs during high-flexion activities: a finite element study. J. Bone Joint Surg. Am. 87 (2), 120–124.
Mulholland, S.J., Wyss, U.P., 2001. Activities of daily living in non-Western cultures: range of motion requirements for hip and knee joint implants. Int. J. Rehabil. Res. 24, 191–198.
Nagura, T., Dyrby, C.O., Alexander, E.J., Andriacchi, T.P., 2002. Mechanical loads at the knee joint during deep flexion. J. Orthop. Res. 20, 881–886.
Nagura, T., Matsumoto, H., Kiriyama, Y., Chaudhari, A., Andriacchi, T.P., 2006. Tibiofemoral joint contact force in deep knee flexion and its consideration in knee osteoarthritis and joint replacement. J. Appl. Biomech. 22, 305–313.
Smith, S.M., Cockburn, R.A., Hemmerich, A., Li, R.M., Wyss, U.P., 2008. Tibiofemoral joint contact forces and knee kinematics during squatting. Gait Posture 27, 376–386.

Taylor, M., Barrett, D.S., 2003. Explicit finite element simulation of eccentric loading in total knee replacement. Clin. Orthop. Relat. Res., 162–171.
Thambyah, A., 2008. How critical are the tibiofemoral joint reaction forces during frequent squatting in Asian populations? Knee 15, 286–294.
Toutoungi, D.E., Lu, T.W., Leardini, A., Catani, F., O'Connor, J.J., 2000. Cruciate ligament forces in the human knee during rehabilitation exercises. Clin. Biomech. (Bristol, Avon.) 15, 176–187.
Van Eijden, T.M., Kouwenhoven, E., Verburg, J., Weijs, W.A., 1986. A mathematical model of the patellofemoral joint. J. Biomech. 19, 219–229.
Weiss, J.M., Noble, P.C., Conditt, M.A., Kohl, H.W., Roberts, S., Cook, K.F., Gordon, M.J., Mathis, K.B., 2002. What functional activities are important to patients with knee replacements? Clin. Orthop. Relat. Res., 172–188.
Zelle, J., Barink, M., Loeffen, R., De Waal, M.M., Verdonschot, N., 2007. Thigh–calf contact force measurements in deep knee flexion. Clin. Biomech. (Bristol, Avon.) 22, 821–826.
Zheng, N., Fleisig, G.S., Escamilla, R.F., Barrentine, S.W., 1998. An analytical model of the knee for estimation of internal forces during exercise. J. Biomech. 31, 963–967.